Mon. Not. R. Astron. Soc. **000**, 000–000 (0000) Printed 5 February 2008 (MN LATEX style file v2.2)

Oxygen abundances in the most oxygen-rich spiral galaxies

Leonid S. Pilyugin[1], Trinh X. Thuan[2] and José M. Vílchez[3]
[1]*Main Astronomical Observatory of National Academy of Sciences of Ukraine, 27 Zabolotnogo str., 03680 Kiev, Ukraine*
[2]*Astronomy Department, University of Virginia, P.O.Box 3818, University Station, Charlottesville, VA 22903*
[3]*Instituto de Astrofísica de Andalucía, CSIC, Apdo, 3004, 18080 Granada, Spain*

Received 2005 November 28; in original form 2005 July 26

ABSTRACT
Oxygen abundances in the spiral galaxies expected to be richest in oxygen are estimated. The new abundance determinations are based on the recently discovered ff – relation between auroral and nebular oxygen line fluxes in high-metallicity H II regions. We find that the maximum gas-phase oxygen abundance in the central regions of spiral galaxies is 12+log(O/H) $\sim$ 8.75. This value is significantly lower (by a factor $\gtrsim$ 5) than the previously accepted value. The central oxygen abundance in the Milky Way is similar to that in other large spirals.

Key words: galaxies: abundances – ISM: abundances – H II regions

1 INTRODUCTION

The oxygen abundance in spiral galaxies has been the subject of much discussion for a long time. Which spiral galaxy is the oxygen-richest one? And how high is the oxygen abundance in the oxygen-richest galaxies? Due to the presence of radial abundance gradients in the disks of spiral galaxies, the maximum oxygen abundance occurs at their centers. The notation $(O/H)_C = 12+\log(O/H)_{R=0}$ will be used thereafter to denote the central oxygen abundance.

The chemical composition of various samples of spiral galaxies has been discussed in a number of papers (e.g. Vila-Costas & Edmunds 1992; Zaritsky et al. 1994; Garnett et al. 1997; van Zee et al. 1998; Garnett 2002). According to those articles, the oxygen-richest galaxies are: NGC 5194 (M 51) with $(O/H)_C$ = 9.54 (Vila-Costas & Edmunds 1992), NGC 3351 with $(O/H)_C$ = 9.41 (Zaritsky et al. 1994), NGC 3184 with $(O/H)_C$ = 9.50 (van Zee et al. 1998), NGC 6744 with $(O/H)_C$ = 9.64 (Garnett et al. 1997). Different versions of the one-dimensional empirical method, proposed first by Pagel et al. (1979) a quarter of a century ago, have been used for oxygen abundance determinations in those papers. Pilyugin (2000, 2001a,b, 2003) has shown that the oxygen abundances in galaxies determined with the one-dimensional empirical calibrations are significantly overestimated at the high-metallicity end (12 + log O/H > 8.25). This for two reasons. First, the then-existing calibrating points at the high-metallicity end were very few and not reliable. Second, the physical conditions in H II regions cannot be taken into account accurately in one-dimensional calibrations. Pilyugin et al. (2004) have used instead a two-dimensional parametric empirical calibration to derive oxygen abundances for a sample of spiral galaxies which includes NGC 3184, NGC 3351, NGC 5194, and NGC 6744. They found generally lower oxygen abundances with $(O/H)_C \sim$ 9.0.

Here we consider anew the problem of the maximum oxygen abundance in spiral galaxies by attempting to derive more accurate oxygen abundances. These can be derived via the classical T_e – method, T_e being the electron temperature of the H II region. Measurements of the auroral lines, such as [OIII]λ4363, are necessary to determine T_e. Unfortunately, they are very faint and often drop below the detectability level in the spectra of high-metallicity H II regions. Pilyugin (2005) has advocated that the faint auroral line flux can be computed from the fluxes in the strong nebular lines via the ff – relation. Then, using the obtained flux in the auroral line, accurate oxygen abundances can be derived using the classical T_e – method. We will estimate $(O/H)_C$ in the spiral galaxies reported to be the oxygen-richest ones, NGC 3184, NGC 3351, NGC 5194, and NGC 6744. For comparison, we will also consider NGC 2903, NGC 2997, NGC 5236 as well the Milky Way Galaxy.

We describe the method used to determine oxygen abundances in H II regions in Section 2. The oxygen abundances in the spiral galaxies NGC 3184, NGC 3351, NGC 5194, NGC 6744, NGC 2903, NGC 2997, NGC 5236 and the Milky Way Galaxy are determined in Section 3. We discuss the reliability of the derived abundances and summarize our conclusions in Section 4.

For the line fluxes, we will be using the following notations throughout the paper: $R_2 = I_{[OII]\lambda3727+\lambda3729}/I_{H\beta}$, $R_3 = I_{[OIII]\lambda4959+\lambda5007}/I_{H\beta}$, $R = I_{[OIII]\lambda4363}/I_{H\beta}$, $R_{23} = R_2 + R_3$. With these definitions, the excitation parameter P can then be expressed as: $P = R_3/(R_2+R_3)$.

2 ABUNDANCE DERIVATION

2.1 Adopted equations for the T_e method

A two-zone model for the temperature structure within the H II region was adopted. Izotov et al. (2005) have recently published a set of equations for the determination of the oxygen abundance in H II regions for a five-level atom. According to those authors, the electron temperature t_3 within the [O III] zone, in units of 10^4K, is given by the following equation

$$t_3 = \frac{1.432}{\log(R_3/R) - \log C_{\rm T}} \quad (1)$$

where

$$C_{\rm T} = (8.44 - 1.09\,t_3 + 0.5\,t_3^2 - 0.08\,t_3^3)\,v \quad (2)$$

$$v = \frac{1 + 0.0004\,x_3}{1 + 0.044\,x_3} \quad (3)$$

and

$$x_3 = 10^{-4} n_e t_3^{-1/2}. \quad (4)$$

As for the ionic oxygen abundances, they are derived from the following equations

$$12 + \log(O^{++}/H^+) = \log(I_{[OIII]\lambda4959+\lambda5007}/I_{H_\beta}) + 6.200 + \frac{1.251}{t_3} - 0.55\log t_3 - 0.014\,t_3, \quad (5)$$

$$12 + \log(O^{+}/H^+) = \log(I_{[OII]\lambda3727+\lambda3729}/I_{H_\beta}) + 5.961 + \frac{1.676}{t_2} - 0.40\log t_2 - 0.034\,t_2 + \log(1 + 1.35x_2). \quad (6)$$

$$x_2 = 10^{-4} n_e t_2^{-1/2}. \quad (7)$$

Here n_e is the electron density in cm^{-3}.

The total oxygen abundances are then derived from the following equation

$$\frac{O}{H} = \frac{O^+}{H^+} + \frac{O^{++}}{H^+}. \quad (8)$$

The electron temperature t_2 of the [O II] zone is usually determined from an equation which relates t_2 to t_3, derived by fitting H II region models. Several versions of this t_2 – t_3 relation have been proposed. A widely used relation has been suggested by Campbell et al. (1986) (see also Garnett (1992)) based on the H II region models of Stasińska (1982). Campbell et al. (1986) has found that the $t_2 - t_3$ relationship can be parameterized as

$$t_2 = 0.7\,t_3 + 0.3. \quad (9)$$

It will be used here.

2.2 The ff – relation

The fluxes R in the auroral lines are necessary to derive the oxygen abundances in H II regions using the T_e method. But they are faint and often undetectable in spectra of high-metallicity H II regions. It was shown (Pilyugin 2005) that the flux R in the auroral line is related to the total flux R_{23} in the strong nebular lines through a relation of the type

$$\log R = a + b \times \log R_{23}. \quad (10)$$

Eq.(10) will be hereinafter referred to as the flux – flux or ff – relation. It was found that this relationship is metallicity-dependent at low metallicities, but becomes independent of metallicity (within the uncertainties of the available data) at metallicities higher than 12+logO/H $\sim$ 8.25, i.e. there is one-to-one correspondence between the auroral and nebular oxygen line fluxes in spectra of high-metallicity H II regions. Pilyugin (2005) derived

$$\log R = -4.264 + 3.087\,\log R_{23}. \quad (11)$$

We can now make use of the ff – relation to define a "discrepancy index", equal to the difference between the logarithm of the observed flux $R^{\rm obs}$ in the [O III]λ4363 line and that of the flux $R^{\rm cal}$ of that line derived from the strong [O II]λ3727, [O III]$\lambda\lambda$4959,5007 lines using the ff - relation:

$$D_{\rm ff} = \log R^{\rm obs} - \log R^{\rm cal}. \quad (12)$$

Since $R_{23} = R_3/P$, the ff – relation can be also expressed in the form R=f(R_3,P). We will consider an expression of the type

$$\log R = a_1 + a_2\,\log P + a_3\,\log R_3 + a_4\,(\log P)^2. \quad (13)$$

Using a sample of H II regions with recent high-precision measurements of oxygen lines fluxes, the values of the coefficients in Eq.(13) can be derived. Such a sample has been compiled by Pilyugin (2005). Bresolin et al. (2004) have recently detected the auroral lines [S III]λ6312 and/or [N II]λ5755 and determined T_e-based abundances in 10 faint H II regions in the spiral galaxy M 51. Unfortunately they were unable to detect the oxygen auroral line. Using the electron temperature t_3 recommended by Bresolin et al. (2004) and the equations given above for the T_e-method, we have estimated the value of R which corresponds to the t_3 for every H II region. It has been found (Pilyugin 2005) that the oxygen line fluxes in six faint H II regions in the spiral galaxy M 51 (CCM 54, CCM 55, CCM 57, CCM 57A, CCM 71A, and CCM 84A) satisfy the ff – relation. These data are included in the present sample to enlarge the ranges in P and R_3. Thus, our sample consists of a total of 48 data points.

The values of the coefficients in Eq.(13) are derived by using an iteration procedure. In the first step, the relation is determined from all data using the least-square method. Then, the point with the largest deviation is rejected, and a new relation is derived. The iteration procedure is pursued until two successive relations have all their coefficients differing by less 0.001 and the absolute value of the largest deviation is less than 0.1 dex. The following ff – relation was obtained

$$\log R = -4.151 - 3.118\,\log P + 2.958\,\log R_3 - 0.680\,(\log P)^2. \quad (14)$$

2.3 Characteristics of the ff – relation

The top panel in Fig. 1 shows the flux R in the oxygen auroral line as a function of the flux R_3 in strong nebular [O III]λ4959 + λ5007 lines. The open and filled circles show individual H II regions with 12+logO/H > 8.25. The relations corresponding to Eq.(14) for different values of the excitation parameter are shown by the solid (P = 1.0), long-dashed (P = 0.7), short-dashed (P = 0.3), and dotted (P =

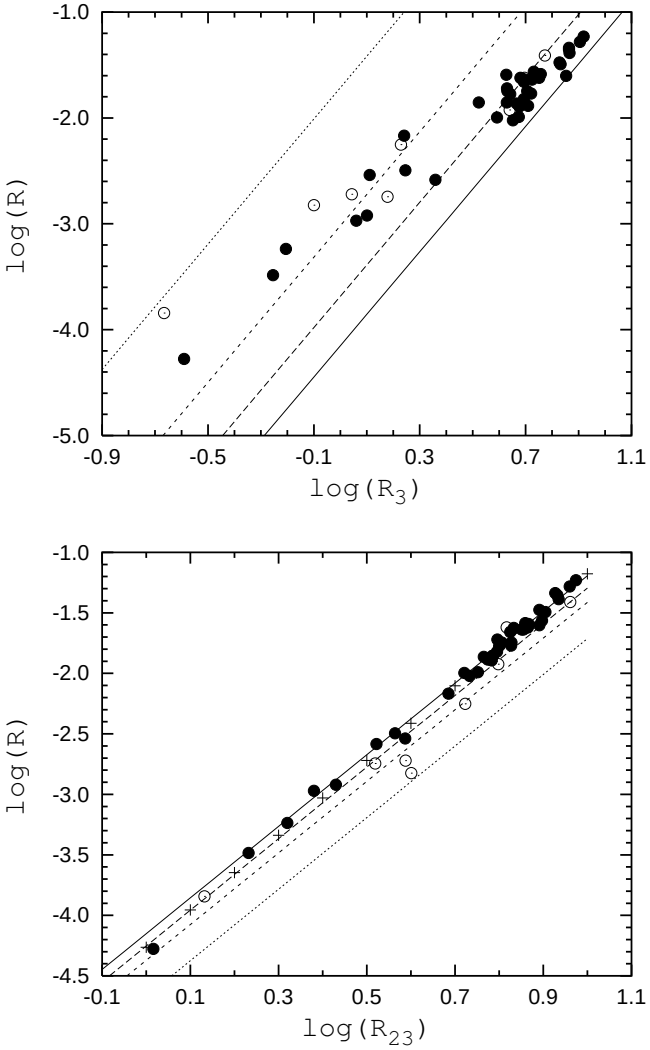

Figure 1. The ff – relations for H II regions. *Top panel.* Flux R in the oxygen auroral line as a function of the flux R_3 in the strong nebular [O III]λ4959 + λ5007 lines for H II regions. The circles (open and filled) show H II regions with 12+logO/H > 8.25. The relations corresponding to Eq.(14) for different values of the excitation parameter are shown by the solid (P = 1.0), long-dashed (P = 0.7), short-dashed (P = 0.3), and dotted (P = 0.1) lines. Only filled circles are used in deriving Eq.(14). *Bottom panel.* Flux R in the oxygen auroral line as a function of the total flux R_{23} in the strong nebular [O II]λ3727 + λ3729 and [O III]λ4959 + λ5007 lines. The open and filled circles have the same meaning as in the top panel. The relations corresponding to Eq.(14) for different values of the excitation parameter are shown by the solid (P = 1.0), long-dashed (P = 0.3), short-dashed (P = 0.2), and dotted (P = 0.1) lines. The relation corresponding to Eq.(11) is shown by plus signs.

0.1) lines. The filled circles show the data used in deriving Eq.(14) (40 out of 48 original data points).

The deviations from the ff – relation given by Eq.(14) as parameterized by the discrepancy index D_{ff} are shown in Fig. 2 as a function of oxygen abundance (top panel) and of excitation parameter P (bottom panel). The filled circles are H II regions used in deriving Eq.(14). The open circles are the other H II regions. Fig. 2 shows that the deviations

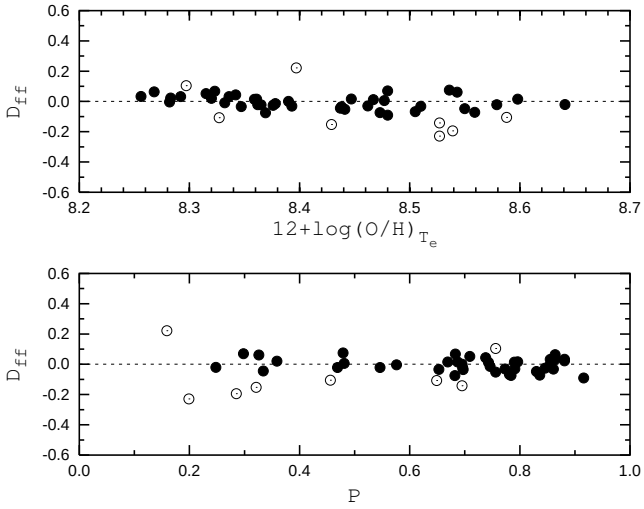

Figure 2. Deviations from the ff – relation as parameterized by the discrepancy index D_{ff} as a function of oxygen abundance (*top panel*) and of excitation parameter P (*bottom panel*). The filled circles are H II regions used in deriving the ff – relation. The open circles are other H II regions.

do not show a correlation either with metallicity or with the excitation parameter.

Let us compare the two ff - relations given by Eq.(11) and Eq.(14). The bottom panel in Fig. 1 shows the flux R in the oxygen auroral line as a function of the total flux R_{23} in strong nebular [O II]λ3727 + λ3729 and [O III]λ4959 + λ5007 lines. The filled circles are the H II regions used in deriving Eq.(14). The open circles are the other H II regions. The relations corresponding to Eq.(14) for different values of the excitation parameter are shown by the solid (P = 1.0), long-dashed (P = 0.3), short-dashed (P = 0.2), and dotted (P = 0.1) lines. The relation corresponding to Eq.(11) is shown by the plus signs. Inspection of the bottom panel of Fig. 1 shows that the relations given by Eq.(14) for values of the excitation parameter P ranging from 1 to $\sim$ 0.3 are close each to other. That led Pilyugin (2005) to conclude that there appears to be no third parameter in the ff – relation. Indeed, examination of the bottom panel in Fig. 1 shows that the ff – relations given by Eq.(11) and Eq.(14) are very similar to each other and reproduce the observational data well at high values of the excitation parameter, P $\gtrsim$ 0.3. At the same time there is an appreciable divergence between those two relations at low values of the excitation parameter, P $\lesssim$ 0.3. For definiteness's sake, we will use the ff – relation given by Eq.(14) for all values of P.

It should be noted however that the particular form of the analytical expression adopted for the ff – relation may be questioned. We have chosen a simple form, Eq.(13), but perhaps a more complex expression may give a better fit to the auroral – nebular oxygen line fluxes relationship. Furthermore, the coefficients in the adopted expression are derived using calibrating H II regions which have a discrepancy index D_{ff} as large as 0.1 dex in absolute value. Perhaps smaller absolute values of D_{ff} may result in a more precise relation. It can be seen that the calibration curves give a satisfactory fit to the observational data. At the same time, Fig. 1 shows that the available measurements for calibrating faint H II regions (those with low R_3) are very few in

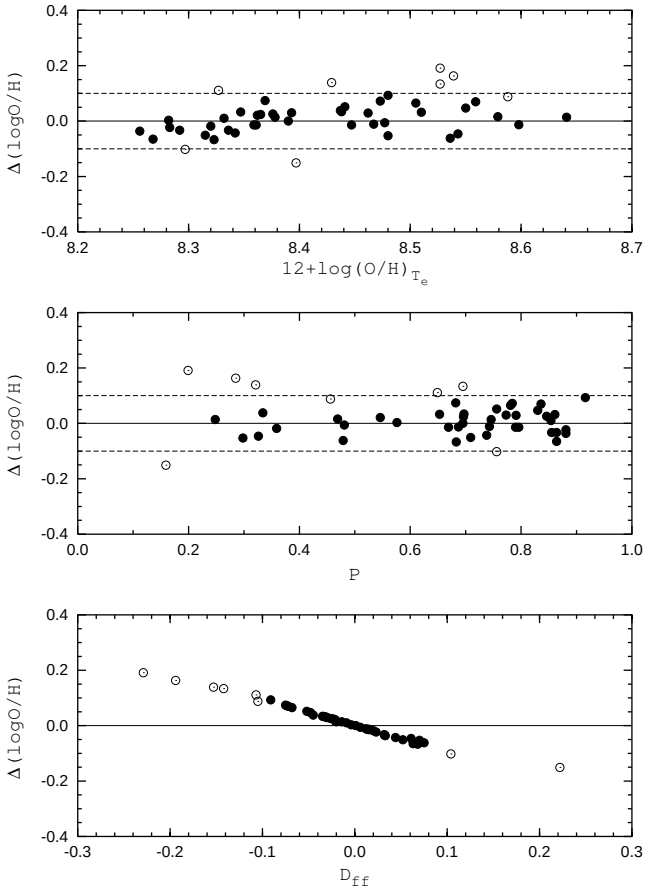

Figure 3. The difference $\Delta\log(O/H) = \log(O/H)_{T_e} - \log(O/H)_{ff}$ as a function of $\log(O/H)_{T_e}$ (*top panel*), of excitation parameter P (*middle panel*), and of discrepancy index D_{ff} (*bottom panel*).

number. Furthermore, the R values for the faint H II regions from Bresolin et al. (2004) are not measured but estimated from the electron temperatures t_3 and, consequently, they are not beyond question. Clearly, high-precision measurements of oxygen lines fluxes in faint H II regions are needed to check the derived ff – relation.

2.4 The $(O/H)_{ff}$ abundances

Using the T_e method, both $(O/H)_{T_e}$ abundances based on the measured line fluxes R^{obs}, and $(O/H)_{ff}$ abundances based on the line fluxes R^{cal} determined from the ff – relation, can be derived for our sample of H II regions. Comparison of their values gives us a check on the $(O/H)_{ff}$ abundances. Fig. 3 shows the difference $\Delta\log(O/H) = \log(O/H)_{T_e} - \log(O/H)_{ff}$ as a function of $\log(O/H)_{T_e}$ (top panel), of excitation parameter P (middle panel), and of discrepancy index D_{ff} (bottom panel). Inspection of Fig. 3 shows that the differences $\Delta\log(O/H)$ do not show an appreciable correlation with metallicity or with excitation parameter. There is however an anticorrelation of $\Delta\log(O/H)$ with D_{ff}. This can be easily understood. The discrepancy index appears to be an indicator of the error in the auroral line R measurements. In that case, positive values of D_{ff} imply overestimated R fluxes, which result in turn in overestimated electron temperatures and underestimated oxygen abundances, i.e. negative $\Delta\log(O/H)$, just the observed trend. In general, the $(O/H)_{ff}$ abundances agree satisfactorily with the $(O/H)_{T_e}$ abundances and do not show any systematic trend.

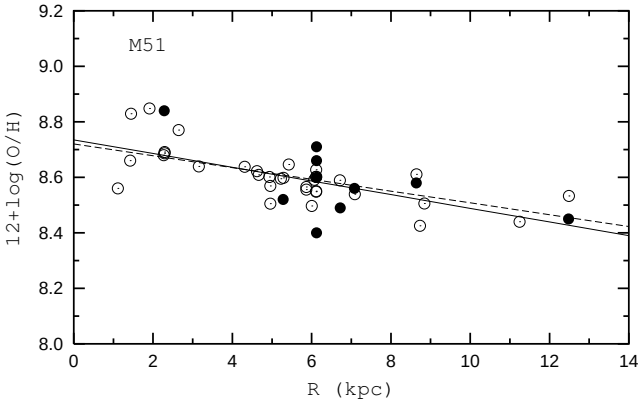

Figure 4. Radial distribution of oxygen abundances in the disk of the spiral galaxy M 51 (NGC 5194). The open circles denote $(O/H)_{ff}$ abundances. The solid line is the linear least-square best fit to those data. The filled circles show $(O/H)_{T_e}$ abundances from Bresolin et al. (2004). The dashed line is their linear regression fit.

In summary, the flux in the faint auroral line [O III]λ4363 can be estimated reasonably well from the measured fluxes in the strong nebular lines [O II]λ3727 + λ3729 and [O III]λ4959 + λ5007 via the ff – relation. Then, using the derived flux in the auroral line, the oxygen abundance can be found through the classic T_e – method.

3 OXYGEN ABUNDANCES IN SPIRAL GALAXIES

Here the derived ff – relation will be applied to derive the oxygen abundances in a number of spiral galaxies. First, M 51 (NGC 5194), the oxygen-richest spiral galaxy ($(O/H)_C$ = 9.54) in the sample of Vila-Costas & Edmunds (1992) will be considered. The value of $(O/H)_C$ in M 51 was derived recently from determinations of $(O/H)_{T_e}$ abundances in a number of H II regions by Bresolin et al. (2004). Comparison between the radial distributions of $(O/H)_{T_e}$ and $(O/H)_{ff}$ abundances in the disk of M 51 provides another possibility to test the reliability of the latter. Second, $(O/H)_{ff}$ abundances in NGC 3184, NGC 3351, and NGC 6744 which have been reported to be the most oxygen-rich spirals, will be determined. Third, we will consider three well-observed spiral galaxies NGC 2903, NGC 2997, and NGC 5236 for comparison. Fourth, the ff – relation will be applied to Galactic H II regions to select high-precision measurements.

3.1 Oxygen abundances in M 51

The compilation of published spectra of H II regions in M 51 is taken from Pilyugin et al. (2004). The H II regions with measured R_3 and R_2 fluxes from Bresolin et al. (2004) (their Tables 1 and 6) have been added. We determine $(O/H)_{ff}$ abundances for every H II region using the derived ff – relation. The $(O/H)_{ff}$ abundances in the H II regions of M 51 are shown as a function of galactocentric distance in Fig. 4

by open circles. The solid line is the linear least-square best fit to those data:

$$12 + \log(O/H) = 8.74\,(\pm0.03) - 0.025\,(\pm0.004) \times R. \quad (15)$$

The distance of M 51 (d = 7.64 Mpc) and the isophotal radius (R_{25} = 5.61 arcmin) were taken from Pilyugin et al. (2004). The filled circles are $(O/H)_{T_e}$ abundances determined by Bresolin et al. (2004). The dashed line is their linear regression:

$$12 + \log(O/H) = 8.72\,(\pm0.09) - 0.02\,(\pm0.01) \times R. \quad (16)$$

Fig. 4 shows that the radial distribution of $(O/H)_{ff}$ abundances agrees well with that of the $(O/H)_{T_e}$ abundances (compare also Eq.(15) and Eq.(16)). This is a strong argument in favor of the reliability of the $(O/H)_{ff}$ abundances.

Some H II regions show large deviations from the general radial trend in oxygen abundances. Some of those deviations can be real, but some are probably caused by uncertainties in the oxygen abundance determinations. It should be emphasized that the uncertainties in the $(O/H)_{ff}$ abundances are not necessarily caused by uncertainties in the line flux measurements. It has been noted (Pilyugin 2005) that the ff – relation gives reliable results only if two conditions are satisfied; *i*) the measured fluxes reflect their relative contributions to the radiation of the whole nebula, and *ii*) the H II region is ionization-bounded. If these two conditions are not met, then the derived $(O/H)_{ff}$ abundances may be significantly in error.

3.2 Oxygen abundances in the most oxygen-rich spiral galaxies

The compilation of published spectra of H II regions in the spiral galaxies NGC 3184, NGC 3351, and NGC 6744 was taken from Pilyugin et al. (2004). The $(O/H)_{ff}$ abundances in the H II regions of NGC 3184 is shown as a function of galactocentric distance in the top panel of Fig. 5. The solid line is the linear least-square best fit to those data:

$$12 + \log(O/H) = 8.73\,(\pm0.03) - 0.035\,(\pm0.004) \times R. \quad (17)$$

The same data are shown for the H II regions of NGC 3351 in the middle panel of Fig. 5. The solid line is the linear least-square best fit to those data:

$$12 + \log(O/H) = 8.74\,(\pm0.02) - 0.023\,(\pm0.004) \times R. \quad (18)$$

Similarly, the data for the H II regions of NGC 6744 are shown in the bottom panel of Fig. 5. The linear least-square best fit to those data is given by:

$$12 + \log(O/H) = 8.75\,(\pm0.04) - 0.022\,(\pm0.003) \times R. \quad (19)$$

The distances of the galaxies and the galactocentric distances of the H II regions were taken from Pilyugin et al. (2004).

Figs. 4 and 5 (see also Eqs.(15,17, 18,19)) show that the values of $(O/H)_C$ in these spiral galaxies are ~ 8.75.

3.3 Oxygen abundances in other spiral galaxies

We will consider here three well-observed spiral galaxies for comparison. The compilation of the published spectra of H II regions in the spiral galaxies NGC 2903, NGC 2997, and NGC 5236 was taken from Pilyugin et al. (2004). Recent measurements from Bresolin et al. (2005) have been added. Oxygen abundances were calculated for every H II region using the derived ff – relation.

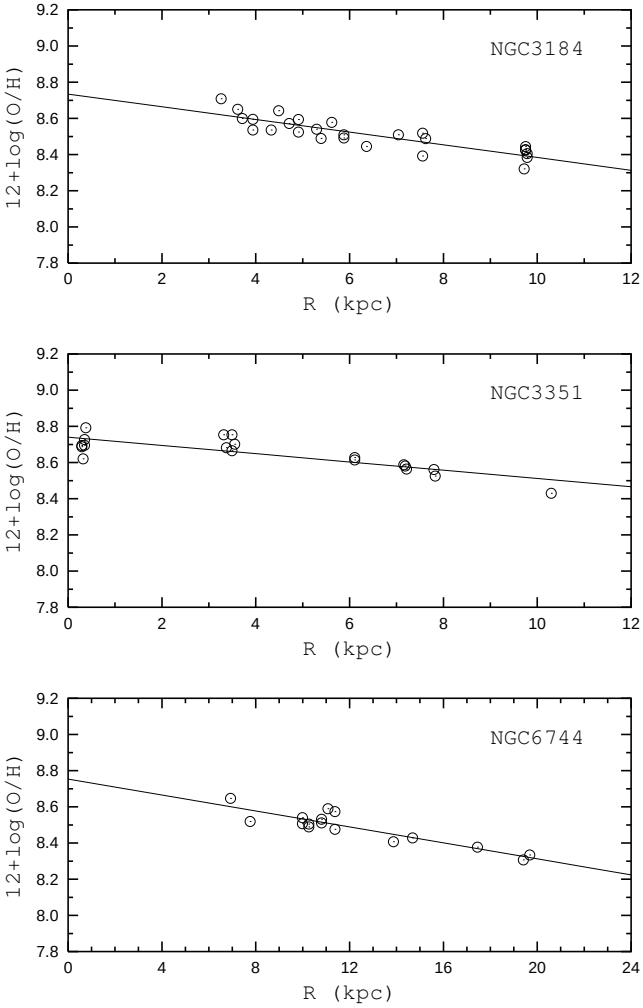

Figure 5. Radial distributions of $(O/H)_{ff}$ abundances in the spiral galaxies NGC 3184, NGC 3351, and NGC 6744. The open circles show individual H II regions. The lines are the least-square fits to those data.

The $(O/H)_{ff}$ abundances in the H II regions of NGC 2903 are shown as a function of galactocentric distance in the top panel of Fig. 6. The solid line is the linear least-square best fit to those data:

$$12 + \log(O/H) = 8.68\,(\pm0.02) - 0.026\,(\pm0.003) \times R. \quad (20)$$

The middle panel of Fig. 6 shows the same for NGC 2997. The linear least-square fit to those data is:

$$12 + \log(O/H) = 8.59\,(\pm0.05) - 0.021\,(\pm0.007) \times R. \quad (21)$$

The data for NGC 5236 are shown in the bottom panel of Fig. 6. The linear least-square fit to those data is:

$$12 + \log(O/H) = 8.62\,(\pm0.01) - 0.022\,(\pm0.005) \times R. \quad (22)$$

The distances of the galaxies were taken from Pilyugin et al. (2004).

Fig. 6 (see also Eqs.(20,21,22)) shows that the $(O/H)_C$

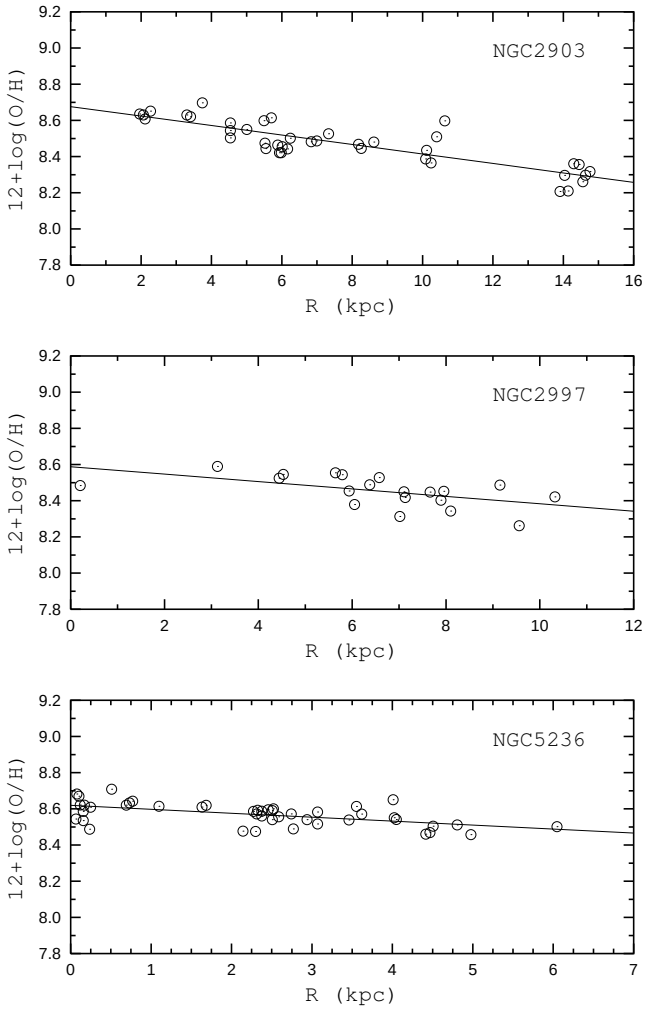

Figure 6. Radial distributions of $(O/H)_{ff}$ abundances in the spiral galaxies NGC 2903, NGC 2997, and NGC 5236. The open circles show individual H II regions. The lines are the least-square fits to those data.

abundances in NGC 2903, NGC 2997, and NGC 5236 are smaller than 8.70, i.e. lower than in NGC 3184, NGC 3351, NGC 5194, and NGC 6744.

Thus, the maximum gas-phase oxygen abundance in the oxygen-richest spiral galaxies is 12+log(O/H) $\sim$ 8.75. This value is significantly lower (by a factor of 5 or more) than the previous value based on the one-dimensional empirical calibrations (e.g. Vila-Costas & Edmunds 1992; Zaritsky et al. 1994; van Zee et al. 1998; Garnett 2002).

3.4 Oxygen abundances in the Milky Way Galaxy

We now consider the Milky Way Galaxy. A compilation of published spectra of Galactic H II regions with an auroral [O III]λ4363 line has been carried out by Pilyugin et al. (2003). That list contains 69 individual measurements of 13 H II regions in the range of galactocentric distances from 6.6 to 14.8 kpc. Recent measurements of six Galactic H II regions by Esteban et al. (2005) were added to that list, resulting in a total of 75 measurements. The T_e-based oxygen abundances were estimated using the equations above.

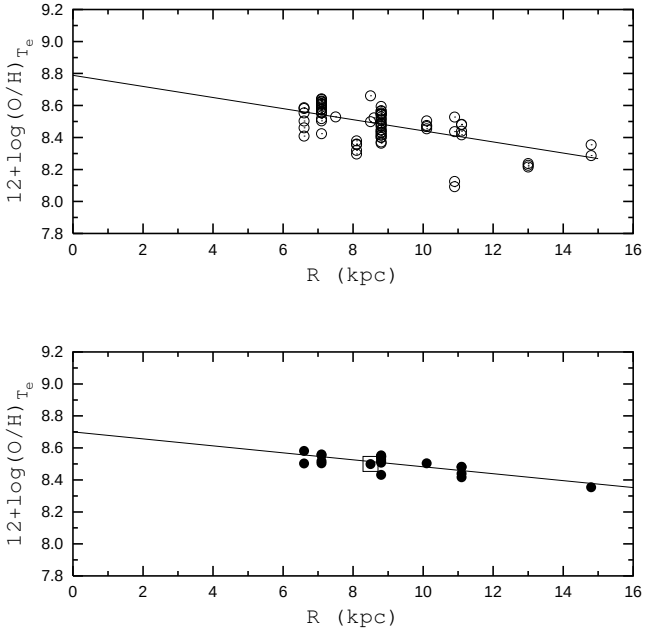

Figure 7. Radial distribution of $(O/H)_{T_e}$ abundances in the disk of the Milky Way Galaxy. *Top panel.* The open circles show $(O/H)_{T_e}$ for all H II regions. The solid line is the linear least-square fit to those data. *Bottom panel.* The filled circles show $(O/H)_{T_e}$ abundances for H II regions with an absolute value of the discrepancy index D_{ff} less than 0.05 dex. The solid line is the linear least-square fit to those data. The open square shows the oxygen abundance in the interstellar gas at the solar galactocentric distance.

The derived $(O/H)_{T_e}$ abundances are shown as a function of galactocentric distance by the open circles in the top panel of Fig. 7. The linear least-square best fit to those data (with two points with a deviation more than 0.2 dex rejected)

$$12 + \log(O/H) = 8.79\,(\pm0.05) - 0.034\,(\pm0.005) \times R \qquad (23)$$

is shown by the solid line in the top panel of Fig. 7.

There is a relative large number of measurements of abundances in the Milky Way Galaxy. They show a large scatter since the quality of the data obtained over a period of more than thirty years is necessarily heterogeneous. Some measurements have a low accuracy. The ff – relation provides a way to select out the H II regions with high quality measurements (Pilyugin & Thuan 2005). The bottom panel of Fig. 7 shows the $(O/H)_{T_e}$ abundances as a function of galactocentric distance for objects with an absolute value of the discrepancy index D_{ff} less than 0.05 dex. The linear least-square best fit to those data

$$12 + \log(O/H) = 8.70\,(\pm0.04) - 0.022\,(\pm0.004) \times R \qquad (24)$$

is shown by the solid line in the bottom panel of Fig. 7. The open square is the oxygen abundance of the interstellar gas at the solar galactocentric distance (see below).

The central oxygen abundance in the Milky Way obtained here, $(O/H)_C \sim 8.70$, is significanly lower than the widely used $(O/H)_C = 9.38$ of Shaver et al. (1983). Our oxygen abundance radial gradient is in agreement with that of Daflon & Cunha (2004). They derived the relation

$$12 + \log(O/H) = 8.762\,(\pm0.105) - 0.031\,(\pm0.012) \times R \quad (25)$$

from abundance determinations in young OB stars.

We note that the central oxygen abundance obtained here for the Milky Way is close to that in other large spirals.

4 DISCUSSION AND CONCLUSIONS

The $(O/H)_{ff}$ abundances determined here rely on the validity of the classic T_e – method. This has been questioned for the high-metallicity regime in a number of investigations by comparison with H II region photoionization models. One should keep in mind however that the existing numerical models of H II regions are far from being perfect (Stasińska 2004), and, hence, the statement that H II region models provide more realistic abundances as compared to the T_e – method should not be taken for granted (Pilyugin 2003). Recently Stasińska (2005) has examined the biases involved in T_e-based abundance determinations at high metallicities. She has found that, as long as the metallicity is low, the derived $(O/H)_{T_e}$ value is very close to the real one. Discrepancies appear around 12+log(O/H) = 8.6 - 8.7, and may become very large as the metallicity increases (Fig. 1a in Stasińska 2005). The derived $(O/H)_{T_e}$ values are smaller than the real ones, sometimes by enormous factors. This means that, if such metal-rich H II regions exist, the classic T_e – method will always lead to systematically lower derived oxygen abundances.

Can the effect discussed by Stasińska be responsible for the low $(O/H)_{T_e}$ abundances obtained here? Let us assume that it is the case, and that the true central oxygen abundances in the spiral galaxies are higher than 12 + log(O/H) = 9.0. What radial distributions of $(O/H)_{T_e}$ abundances in the disk of spiral galaxies would one expect in this case? Starting from the periphery of a galaxy, the $(O/H)_{T_e}$ abundances would increase with decreasing galactocentric distance (following the true abundances) until the $(O/H)_{T_e}$ abundance reaches the value of 12+log(O/H) $\sim$ 8.7. After that the $(O/H)_{T_e}$ abundances would decrease with decreasing galactocentric distance because of the Stasińska (Fig. 1a in Stasińska 2005) effect, although the true abundances continue to increase with decreasing galactocentric distance. Thus, the radial distribution of $(O/H)_{T_e}$ abundances should show a bow-shaped curve with a maximum value of 12+log(O/H) $\sim$ 8.7 at some galactocentric distance.

Do the actual data (Fig. 5–7) show such a behavior? The derived radial distributions of $(O/H)_{T_e}$ abundances in the disks of spiral galaxies do not show an appreciable curvature, and the $(O/H)_{T_e}$ abundances increase more or less monotonically with decreasing galactocentric distance. Only the H II regions in the very central parts of the spiral galaxies NGC 3351 (the middle panel of Fig. 5) and NGC 2997 (the middle panel of Fig. 6) may show $(O/H)_{T_e}$ abundances which are slightly lower than expected from the general radial abundance trends, but the effect is very slight and may not be real if errors of 0.1 dex (Fig. 3) in the calibration and in the line intensity measurements are taken into account. To settle the question of whether the abundances in the metal-richest H II regions are affected by the Stasińska's effect, many more accurate measurements of H II regions (including those in the very central parts) in the most oxygen-rich spiral galaxies are necessary.

Thus, while our results do not rule out the possible existence of the Stasińska's effect, they suggest that the great majority of H II regions in galaxies are in a metallicity range where this effect is not important. Indeed, the Stasińska's effect becomes important only at oxygen abundances higher than 12 + log(O/H) $\sim$ 8.7. We have found that this "critical" value is reached only in the central part of the most oxygen-rich galaxies. We conclude that, in the light of our present results, H II regions with 12+log(O/H) > 8.7 are rare, if they exist at all. It should be noted that Stasińska also questioned the existence of such metal-rich H II regions (Section 2.2 in Stasińska 2005).

Another factor that can affect T_e-based abundance determinations is the temperature fluctuations inside H II regions (Peimbert 1967). If they are important, the $(O/H)_{T_e}$ abundance would be a lower limit. In most cases the effect appears to be small, probably under 0.1 dex (Pagel 2003).

Fortunately, there is a way to verify the validity of the T_e – method at high metallicities (Pilyugin 2003). High-resolution observations of the weak interstellar OIλ1356 absorption lines towards stars allow one to determine the interstellar oxygen abundance in the solar vicinity with a very high precision. It should be noted that this method is model-independent. These observations yield a mean interstellar oxygen abundance of 284 – 390 O atoms per 10^6 H atoms (or 12+log(O/H) = 8.45 – 8.59) (Meyer et al. 1998; Sofia & Meyer 2001; Cartledge et al. 2004). Oliveira et al. (2005) have determined a mean O/H ratio of 345 $\pm$19 O atoms per 10^6 H atoms (or 12+log(O/H) = 8.54) for the Local Bubble. Thus, an oxygen abundance 12+log(O/H) = 8.50 in the interstellar gas at the solar galactocentric distance seems to be a reasonable value. The value of the oxygen abundance at the solar galactocentric distance traced by $(O/H)_{T_e}$ abundances in H II regions is then in good agreement with the oxygen abundance derived with high precision from the interstellar absorption lines towards stars (open square in the bottom panel of Fig. 7). This is strong evidence that the classic T_e – method provides accurate oxygen abundances in high-metallicity H II regions.

The measured oxygen abundance in the solar vicinity provides an indirect way to check our derived central oxygen abundances. The oxygen abundance in the solar vicinity is 12+log(O/H)=8.50, and a gas mass fraction $\mu \sim 0.20$ seems appropriate. The simple model of chemical evolution of galaxies predicts that a decrease of μ by 0.1 results in a increase of the oxygen abundance by $\sim$ 0.12 dex in the range of μ from $\sim$ 0.75 to $\sim$ 0.05. When all the gas in the solar vicinity will be converted into stars, the oxygen abundance will increase by 0.2 – 0.25 dex and will reach a value around 12+log(O/H) = 8.70 – 8.75. This value is in excellent agreement with the central oxygen abundances obtained above for the Milky Way and other galaxies. There is no room for central oxygen abundances as large as 12+logO/H = 9.00 or greater.

The present study suggests that there is an upper limit to the oxygen abundances in spiral galaxies. If true, the existing luminosity – metallicity relation should be revisited. One can expect the metallicity to increase with luminosity up to 12+(O/H) $\sim$ 8.75, but to remain approximately constant for higher metallicities, resulting in a flattening of the luminosity – metallicity relation. This suggestion will be investigated in a future paper.

The maximum gas-phase oxygen abundance in spiral

galaxies is 12+log(O/H) $\sim$ 8.75. The central oxygen abundance in the Milky Way is similar to that in other large spirals. Some fraction of the oxygen is locked into dust grains in H II regions. Esteban et al. (1998) found that the fraction of the dust-phase oxygen abundance in the Orion nebula is about 0.08 dex. Then, the true gas+dust maximum value of the oxygen abundance in H II regions of spiral galaxies is 12+log(O/H) $\sim$ 8.85. This value can increase up to $\sim$ 8.90 – 8.95 if temperature fluctuations inside H II regions are important.

Acknowledgments

We thank Yuri Izotov and Grazyna Stasińska for providing us with a new set of T_e-equations in advance of publication. We thank the anonymous referee for helpful comments. The research described in this publication was made possible in part by Award No UP1-2551-KV-03 of the U.S. Civilian Research & Development Foundation for the Independent States of the Former Soviet Union (CRDF). L.S.P was also partly supported by grant No 02.07/00132 from the Ukrainian Fund of Fundamental Investigations.

REFERENCES

Bresolin, F., Garnett, D.R., & Kennicutt, R.C. 2004, ApJ, 615, 228
Bresolin, F., Schaerer, D., González Delgado, R.M., & Stasińska, G. 2005, A&A, 441, 981
Campbell, A., Terlevich, R., & Melnick, J. 1986, MNRAS, 223, 811
Cartledge, S.I.B., Lauroesch, J.T., Meyer, D.M. & Sofia, U.J., 2004, ApJ, 613, 1037
Daflon, S. & Cunha, K. 2004, AJ, 617, 1115
Esteban, C., Peimbert, M., Torres-Peimbert, S. & Escalante, V. 1998, MNRAS, 295, 401
Esteban, C., García-Rojas, J., Peimbert, M., Peimbert, A., Ruiz, M.T., Rodríguez, M., & Carigi, L. 2005, ApJ, 618, L95
Garnett, D.R. 1992, AJ, 103, 1330
Garnett, D.R. 2002, ApJ, 581, 1019
Garnett, D.R., Shields, G.A., Skillman, E.D., Sagan, S.P., & Dufour, R.J. 1997, ApJ, 489, 63
Izotov, Y.I., Stasińska, G., Meynet, G., Guseva, N.G., & Thuan, T.X. 2005, A&A, in press (astro-ph/0511644)
Kennicutt, R.C., Bresolin, F., & Garnett, D.R. 2003, ApJ, 591, 801
Meyer D.M., Jura M., & Cardelli J.A. 1998, ApJ, 493, 222
Oliveira, C.M., Dupuis, J., Chayer, P., & Moss, H.W. 2005, ApJ, 625, 232
Pagel, B.E.J. 2003, in: CNO in the Universe, Eds. C. Charbonnel, D. Schaerer, & G. Meynett, (ASP Conference Series No 304), p. 187
Pagel, B.E.J., Edmunds, M.G., Blackwell, D.E., Chun, M.S., & Smith, G. 1979, MNRAS, 189, 95
Peimbert, M. 1967, ApJ, 150, 825
Pilyugin, L.S. 2000, A&A, 362, 325
Pilyugin, L.S. 2001a, A&A, 369, 594
Pilyugin, L.S. 2001b, A&A, 373, 56
Pilyugin, L.S. 2003, A&A, 399, 1003
Pilyugin, L.S. 2005, A&A, 436, 1L
Pilyugin, L.S., Ferrini, F., & Shkvarun, R.V., 2003, A&A, 401, 557
Pilyugin, L.S. & Thuan, T.X. 2005, ApJ, 631, 231
Pilyugin, L.S., Vílchez, J.M., & Contini, T. 2004, A&A, 425, 849
Shaver, P.A., McGee, R.X., Newton, L.M., Danks, A.C., Pottash, S.R. 1983, MNRAS, 204, 53
Sofia U.J., & Meyer D.M. 2001, ApJL, 554, 221L
Stasińska, G. 1982, A&AS, 48, 299
Stasińska, G. in: Cosmochemistry. The melting pot of the elements. XIII Canary Islands Winter School of Astrophysics. Eds. C., Esteban, R.J., García López, A., Herrero, F., Sánchez, Cambridge contemporary astrohysics, Cambridge, UK, Cambridge University Press, 2004, p. 115
Stasińska, G. 2005, A&A, 434, 507
Vila-Costas, M.B., & Edmunds, M.G. 1992, MNRAS, 259, 121
van Zee, L., Salzer, J.J., Haynes, M.P., O'Donoghue, A.A., & Balonek, T.J. 1998, AJ, 116, 2805
Zaritsky D., Kennicutt R.C., Jr., & Huchra J.P. 1994, ApJ 420, 87